CHEMISTRY OF MATERIALS
Article

Chem. Mater. **2010,** *22,* 4419–4425 4419
DOI:10.1021/cm1010289

Permittivity Enhanced Atomic Layer Deposited HfO_2 Thin Films Manipulated by a Rutile TiO_2 Interlayer

Minha Seo, Seong Keun Kim, Jeong Hwan Han, and Cheol Seong Hwang*

WCU Hybrid Materials Program, Department of Materials Science and Engineering and Inter-University Semiconductor Research Center, Seoul National University, Seoul, 151-742, Korea

Received April 13, 2010. Revised Manuscript Received June 18, 2010

HfO_2/TiO_2 bilayered thin films were grown on Ru and TiN electrodes at 250 °C by atomic layer deposition. The crystalline structure of the HfO_2 layer was affected by the crystalline structure of the TiO_2 under-layer. The HfO_2 layer grown on an anatase-structured TiO_2 layer crystallized into a monoclinic structure with a dielectric constant of ~16, whereas the HfO_2 layer grown on rutile-structured TiO_2 contained a mixture of tetragonal (or cubic) and amorphous phases. This mixed structured-HfO_2 film had a higher dielectric constant of ~29. The formation of tetragonal HfO_2 on the rutile structured TiO_2 resulted from the structural compatibility of the specific planes of the tetragonal HfO_2 and rutile structured TiO_2. The thin HfO_2 layer with the higher dielectric constant deposited on rutile TiO_2 suppressed the leakage current effectively. Consequently, an equivalent oxide thickness of 0.41 nm from the HfO_2/TiO_2 bilayer (thickness of HfO_2 and TiO_2 was 0.5 and 6 nm, respectively) was achieved with a leakage current of $\sim 2 \times 10^{-7}$ A/cm^2 at an applied voltage of 0.8 V.

I. Introduction

A range of high-dielectric constant (k) materials have recently been examined to further increase the capacitance density of capacitors in dynamic random access memory (DRAM). The capacitance density of a dielectric film can be represented by the equivalent oxide thickness (t_{ox}), which is given as the physical thickness multiplied by ($3.9/k$). The attainable minimum t_{ox} with a sufficiently low leakage current ($< 1 \times 10^{-7}$ A cm^{-2}) is ~0.7 nm from a $ZrO_2/Al_2O_3/ZrO_2$ triple layer that is formed on the TiN electrode.[1,2] However, the technology roadmap indicates that the t_{ox} should be < 0.5 nm for DRAMs with the design rule of < 30 nm.[3] ZrO_2 and Al_2O_3 have k values of ~35 and ~8, respectively, which are unsuitable for further decreasing the t_{ox}. This means that a new dielectric material with a higher k value is needed. For this purpose, Kim et al. and Choi et al. reported that rutile-structured TiO_2 has a very promising high k value (80−130)[4−6] even at thicknesses as low as ~10 nm. However, the lower band gap (~3.1 eV) and Fermi level pinning at a location close to the conduction band edge of undoped TiO_2 has limited the minimum t_{ox} to 0.8 nm.[7] Al-doping is a highly promising method to reduce the leakage current, and the minimum t_{ox} has been decreased to 0.48 nm.[8] However, doped AlO_x has a lower k value, which decreases the bulk dielectric constant of the TiO_2 film.

On the other hand, other dielectric materials with a higher energy gap (E_g, > 5 eV) and high k value can be pursued. k and E_g have an inverse relationship.[9] Therefore, a proper combination of materials with higher E_g and slightly low k and with lower E_g and higher k might be used to achieve a smaller t_{ox} value. Among the various potential candidate materials for the higher E_g with a slightly low k layer, HfO_2 is definitely one of the most promising materials owing to its outstanding properties, such as reasonably high k value and wide band gap (5.68 eV).[10] In addition, the atomic layer deposition (ALD) process is quite mature because of the mass-production of high performance logic chips using HfO_2-based gate dielectric films.[11] Therefore, this study examined the proper combination of these two layers, that is, TiO_2 and HfO_2. Another motivation for this study is described below.

HfO_2 has several crystalline structures, such as monoclinic, tetragonal, cubic, and orthorhombic, all of which have different properties. In particular, the k values of tetragonal and cubic structured HfO_2 are much higher than those of the monoclinic structure. The k value of

*To whom correspondence should be addressed. E-mail: cheolsh@snu.ac.kr.

(1) Kil, D.-S.; Song, H.-S.; Lee, K.-J.; Hong, K.; Kim, J.-H.; Park, K.-S.; Yeom, S.-J.; Roh, J.-S.; Kwak, N.-J.; Sohn, H.-C.; Kim, J.-W.; Park, S.-W. *VLSI Symp. Tech. Dig.* **2006**, 38.
(2) Cho, H. J.; Kim, Y. D.; Park, D. S.; Lee, E.; Park, C. H.; Jang, J. S.; Lee, K. B.; Kim, H. W.; Ki, Y. J.; Han, I. K.; Song, Y. W. *Solid-State Electron.* **2007**, *51*, 1529.
(3) International Technology Roadmap for Semiconductors **2009**.
(4) Kim, S. K.; Kim, W.-D.; Kim, K.-M.; Hwang, C. S.; Jeong, J. *Appl. Phys. Lett.* **2004**, *85*, 4112.
(5) Kim, S. K.; Hwang, G. W.; Kim, W.-D.; Hwang, C. S. *Electrochem. Solid-State Lett.* **2006**, *9*, F5.
(6) Choi, G.-J.; Kim, S. K.; Won, S.-J.; Kim, H. J.; Hwang, C. S. *J. Electrochem. Soc.* **2009**, *156*, G138.
(7) Kim, S. K.; Lee, S. Y.; Seo, M.; Choi, G.-J.; Hwang, C. S. *J. Appl. Phys.* **2007**, *102*, 024109.
(8) Kim, S. K.; Choi, G.-J.; Lee, S. Y.; Seo, M.; Lee, S. W.; Han, J. H.; Ahn, H.-S.; Han, S.; Hwang, C. S. *Adv. Mater.* **2008**, *20*, 1429.
(9) Elliot, S. *The Physics and Chemistry of Solids*; Wiley: New York, 1998.
(10) Balog., M.; Schieber, M. *Thin Solid Films* **1977**, *41*, 247.
(11) http://www.intel.com/technology/45nm/index.htm (accessed Mar 2010).

Published on Web 07/09/2010

monoclinic structured HfO_2 is <20, which is not much different from the value of amorphous HfO_2, whereas the value for cubic and tetragonal structured HfO_2 is expected to be $\sim$30 and $\sim$30−70, respectively.[12−14] Therefore, to scale down the feature size of DRAM cells to <30 nm, the formation of cubic or tetragonal structured HfO_2, not monoclinic HfO_2, is needed to achieve a very low t_{ox}, < 0.5 nm.

ALD is a good method for depositing HfO_2 films for the next generation DRAM application on account of its excellent thickness control, uniform film growth over large areas, excellent conformality on three-dimensional structures, and relatively low growth temperature. However, in the ALD process of HfO_2 films, amorphous HfO_2 thin films are generally grown in the very thin film thickness range (<10 nm), and are usually crystallized into the monoclinic structure at a certain film thickness.[15,16] In the case of ZrO_2, which has similar crystalline structures, a high temperature stable phase, such as cubic or tetragonal phases, is obtained at low growth temperatures (<300 °C) even at very thin film thickness because of the size effect of the small grains[17] or specific precursor chemistry.[18] On the other hand, high temperature stable phases, cubic and tetragonal HfO_2 films, are rarely grown by ALD and even chemical vapor deposition (CVD).[15,16,19] This has been a serious drawback of HfO_2 film as a dielectric for application to the next generation DRAM capacitors.

Although cubic and tetragonal HfO_2 films are barely formed by ALD and CVD, doping impurities into the HfO_2 films achieves the formation of tetragonal or cubic structured HfO_2 films because the impurities can reduce the energy barrier for the formation of high temperature stable phases.[20−25] Adopting amorphous Ta_2O_5 interlayer increased the tendency of transforming the monoclinic HfO_2 into tetragonal HfO_2 in the ALD of HfO_2/Ta_2O_5 nanolaminate film using the $HfCl_4$ precursor at a growth temperature of 325 °C.[20] However, doping of impurities into the films can decrease the k value of the HfO_2 films and retard crystallization. Furthermore, it is generally difficult to crystallize HfO_2 films to cubic or tetragonal structures by doping impurities at very thin film thickness ($<\sim5$ nm),[26] although Niinistö et al. reported that Y-doped HfO_2 film was crystallized even at a thickness of 5 nm.[27] This is because the interfacial energy between the crystallized HfO_2 film and substrate is larger than the decreasing bulk free energy of the HfO_2 film by crystallization. For these reasons the formation of the tetragonal HfO_2 films by doping with impurities may be unsuitable for applications of DRAM capacitor dielectrics, which require an extremely low t_{ox} and leakage current.

Modification of the crystal structural into thermodynamically unstable or metastable phases by local epitaxy with the substrate even for polycrystalline thin film is possible. One of the relevant results can be found from the transformation of the anatase (or brookite) TiO_2 to rutile TiO_2 by the local epitaxy effect of RuO_2 or IrO_2 substrate layer, even at a very low ALD temperature of 250 °C.[4,5,28] Therefore, the effect of the substrate layer, which has structural compatibility with cubic or tetragonal structured HfO_2, was examined for the formation of the HfO_2 films with higher k value. The decrease in interfacial energy between the deposited film and substrate makes it possible to form cubic or tetragonal structured HfO_2 films at relatively low temperatures by the ALD process. Kim et al. reported that rutile-structured TiO_2 films, which are the high temperature ($>\sim700$ °C) stable phase, were grown on a RuO_2 surface at 250 °C because of the structural compatibility between rutile TiO_2 and RuO_2.[4,5] Alternatively, anatase TiO_2, which has a dielectric constant of $\sim$35, can be grown under identical conditions on a TiN electrode.

In this study, rutile TiO_2 and anatase TiO_2 films, which have a different crystal structure but similar chemical properties, were chosen as the substrate layer to control the phase of HfO_2 without doping. The structural and electrical properties of HfO_2 films on the rutile and anatase TiO_2 layers were investigated.

II. Experimental Procedure

HfO_2/TiO_2 films were deposited by ALD at a growth temperature of 250 °C using a traveling-wave type reactor. *t*-Butoxytris(ethylmethylamido)hafnium [$HfO^tBu(NEtMe)_3$, BTEMAH] and tetrakisisopropoxide titanium [$Ti(OC_3H_7)_4$, TTIP] were used as the Hf and Ti precursors, respectively. O_3 with a concentration of 400 g/m^3 was used as the oxygen source. A mixture of O_2/N_2 at a flow rate of 800 sccm/5 sccm was introduced into an O_3 generator to produce O_3. To examine the effect of the crystalline structure of TiO_2 on the structural properties of the HfO_2 upper-layer, the TiO_2 films were grown

(12) Leger, J. M.; Atouf, A.; Tomaszewski, P. E.; Pereira, A. S. *Phys. Rev. B* **1993**, *48*, 93.
(13) Zhao, X.; Vanderbilt, D. *Phys. Rev. B* **2002**, *65*, 233106.
(14) Rignanese, G.-M.; Gonze, X.; Jun, G.; Cho, K.; Pasquarello, A. *Phys. Rev. B* **2004**, *69*, 184301.
(15) Cho, M.; Park, J.; Park, H. B.; Hwang, C. S. *Appl. Phys. Lett.* **2002**, *81*, 334.
(16) Cho, M.; Park, H. B.; Park, J.; Lee, S. W.; Hwang, C. S. *Appl. Phys. Lett.* **2003**, *83*, 5503.
(17) Kim, S. K.; Hwang, C. S. *Electrochem. Solid-State Lett.* **2008**, *11*, G9.
(18) Niinistö, J.; Kukli, K.; Kariniemi, M.; Ritala, M.; Leskelä, M.; Blasco, N.; Pinchart, A.; Lachaud, C.; Laaroussi, N.; Wang, Z.; Dussarrat, C. *J. Mater. Chem.* **2008**, *18*, 5243.
(19) Williams, P. A.; Jones, A. C.; Tobin, N. L.; Chalker, P. R.; Taylor, S.; Marshall, P. A.; Bickley, J. F.; Smith, L. M.; Davies, H. O.; Critchlow, G. W. *Chem. Vap. Deposition* **2003**, *9*, 309.
(20) Kukli, K.; Ihanus, J.; Ritala, M.; Leskela, M. *Appl. Phys. Lett.* **1996**, *68*, 3737.
(21) Ushakov, S. V.; Brown, C.; Navrotsky, A. *J. Mater. Res.* **2004**, *19*, 693.
(22) Neumayer, D. A.; Cartier, E. *J. Appl. Phys.* **2001**, *90*, 1801.
(23) Park, P.; Kang, S.-W. *Appl. Phys. Lett.* **2006**, *89*, 192905.
(24) Triyoso, D. H.; Hegde, R. I.; Schaeffer, J. K.; Roan, D.; Tobin, P. J.; Samavedam, S. B.; White, B. E., Jr. *Appl. Phys. Lett.* **2006**, *88*, 222901.
(25) Lee, C.-K.; Cho, E.; Lee, H.-S.; Hwang, C. S.; Han, S. *Phys. Rev. B* **2008**, *78*, 012102.
(26) Park, T. J.; Kim, J. H.; Jang, J. H.; Lee, C.-K.; Na, K. D.; Lee, S. Y.; Jung, H.-S.; Kim, M.; Han, S.; Hwang, C. S. Chem. Mater., accepted for publication.
(27) Niinistö, J.; Kukli, K.; Sajavaara, T.; Ritala, M.; Leskelä, M.; Oberbeck, L.; Sundqvist, J.; Schrödere, U. *Electrochem. Solid-State Lett.* **2009**, *12*, G1.
(28) Joo, D. K.; Park, J. S.; Kang, S. W. *Electrochem. Solid-State Lett.* **2009**, *12*, H77.

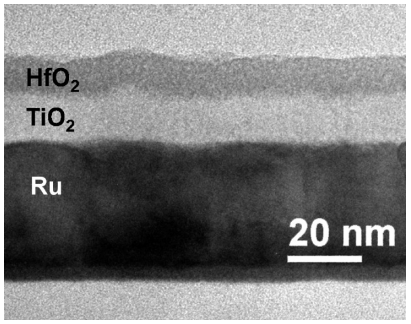

Figure 1. TEM image of a $HfO_2/TiO_2/Ru$ stack film.

on Ru and TiN substrates, corresponding to rutile and anatase structures, respectively. The TiO_2 films on the Ru and TiN substrates were followed by the deposition of HfO_2 films. A cycle for the deposition of HfO_2 was composed of a BTEMAH injection (4.5 s) − Ar purge (5 s)− O_3 injection (3 s) − Ar purge (3 s) steps. The detailed experimental conditions for the deposition of TiO_2 and HfO_2 are reported elsewhere.[4,29]

The film thickness was evaluated by X-ray fluorescence spectroscopy (XRF, Spectrace, QuanX), which was confirmed by the cross-section images from high-resolution transmission electron microscopy (HRTEM, JEOL, 3000F). The crystalline structure of the films was examined by HRTEM and glancing angle X-ray diffraction (GAXRD, PANalytical, X'pert Pro MPD) at an incident angle of 1°. The surface morphology of the films was examined by atomic force microscopy (AFM, JEOL, JSPM5200). A wet etching process for the films was performed using a hydrofluoric acid solution (HF/H_2O = 1:100) to examine the crystallinity of the HfO_2 film on rutile TiO_2.

The electrical properties of the HfO_2/TiO_2 films were examined as follows. Metal−insulator−metal (MIM) capacitors were fabricated by depositing 100 nm-thick Pt films using an electron beam evaporator through a shadow mask for the top electrodes. The area of the Pt electrodes was approximately 6.0×10^4 μm^2, and the accurate area of each measured capacitor was acquired by optical microscopy. The MIM capacitors were annealed at 400 °C under a N_2/O_2 (5%) atmosphere after fabrication of the top electrodes. A Hewlett-Packard 4194A impedance analyzer and 4140B picoammeter were used to measure the capacitance−voltage ($C-V$) and current density−voltage ($J-V$), respectively. The C−V measurement was performed at a frequency of 10 kHz. Five to ten capacitors were measured from each sample to compensate for local variations.

III. Results and Discussions

Fifteen nanometer-thick anatase and rutile TiO_2 films, which may have different interfacial energies with HfO_2, were used as substrates to examine the effect of the TiO_2 under-layer on the crystalline structure of the HfO_2 films grown by ALD. Figure 1 shows a cross-section TEM image of the HfO_2/TiO_2 film grown on a Ru substrate.

Monoclinic HfO_2, which is the thermodynamically stable phase under these deposition conditions, has relatively a low k value (< 20), whereas cubic and tetragonal HfO_2 have higher k values.[13,25] Therefore, the bulk k values of the HfO_2 upper-layer deposited on the two types

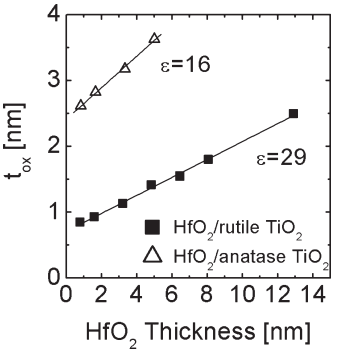

Figure 2. Change in the t_{ox} of HfO_2/rutile TiO_2/Ru films (■) and HfO_2/anatase TiO_2/Ru films (△) as a function of the HfO_2 film thickness.

of TiO_2 under-layer can provide a clue for examining the crystalline structure of HfO_2 films. Figure 2 shows the changes in the t_{ox} of the capacitors with the HfO_2 films on the rutile TiO_2/Ru and anatase TiO_2/TiN substrates as a function of the HfO_2 film thickness. The k value of the HfO_2 films could be calculated from the inverse slopes of the best linear fit ($t_{ox} = (3.9/k) \times t_{phy}$, where t_{phy} means the physical thickness of HfO_2 film). The calculated k value of the HfO_2 films grown on anatase TiO_2 was 16, which is consistent with the k value reported for monoclinic HfO_2.[12−14] Kukli et al. also reported that the incorporation of anatase TiO_2 induced the crystallization of HfO_2 film into the monoclinic structure.[30] On the other hand, the k value of the HfO_2 films on the rutile TiO_2 was 29, suggesting that the HfO_2 films are not composed of a pure monoclinic phase. Considering that the deposition conditions of the HfO_2 films were identical for both films, it is clear that the different structural compatibility between HfO_2 and the rutile and anatase structured TiO_2 is the reason for the different k value of the HfO_2 films. The y-axis intercepts are related to the t_{ox} contribution by the TiO_2 under-layers. The smaller t_{ox} contribution from the TiO_2/Ru stack indicates that the TiO_2 under-layers on the Ru indeed have a higher k value than the films on TiN. The y-intercept suggests that the k value of the 15 nm-thick TiO_2 on Ru and TiN is ~80 and ~25, respectively. The unexpectedly low k value of the anatase TiO_2 film compared to the same film on the Pt electrode (~ 37)[4] suggests that the TiN electrode was oxidized during the ALD of TiO_2.

GAXRD measurements were carried out to confirm the crystal structure of the HfO_2 film with a higher k value on rutile TiO_2. However, no peaks corresponding to monoclinic or other crystal structure HfO_2 were observed from the GAXRD pattern, even at a thick thickness of 29 nm (data not shown). This means that this higher k HfO_2 layer is not fully crystallized and the crystal grains are very small if they do exist. Such a thick HfO_2 upper-layer still has an amorphous portion, whereas the amorphous HfO_2 film deposited directly on the Si substrate had transformed completely to a crystalline phase at thicknesses

(29) Seo, M.; Min, Y.-S.; Kim, S. K.; Park, T. J.; Kim, J. H.; Na, K. D.; Hwang, C. S. *J. Mater. Chem.* **2008**, *18*, 4324.

(30) Kukli, K.; Ritala, M.; Leskelä, M.; Sundqvist, J.; Oberbeck, L.; Heitmann, J.; Schröder, U.; Aarik, J.; AidlaKukli, A. *Thin Solid Films* **2007**, *515*, 6447.

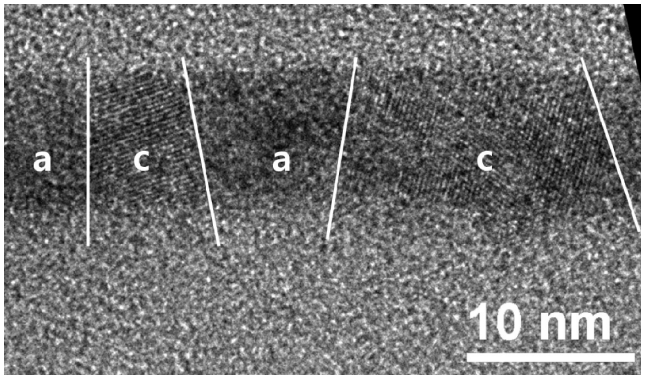

Figure 3. HRTEM image of HfO_2 film deposited on rutile TiO_2 film, which shows a mixed structure of columnar crystal regions (c) and amorphous regions (a).

>18 nm.[29] Because amorphous structured HfO_2 film cannot have such a high k value of 29, some parts of the HfO_2 layer on rutile TiO_2 are believed to be a small grain-sized crystalline phase with a higher k value. The linearity of the graph in Figure 2 was maintained at least up to a HfO_2 film thickness of 14 nm. This suggests that the HfO_2 layer structure does not change along the direction perpendicular to the film surface. In addition, the crystal grains are believed to have grown right on some rutile TiO_2 surface because the crystals with the higher k value could be only formed on the rutile TiO_2 layer. Therefore, the shape of the partially crystallized HfO_2 film is supposed to be a mixed structure of an amorphous matrix and small embedded columnar grains of crystals with a higher k value extending from the HfO_2/TiO_2 interface to the surface. This was confirmed by HRTEM.

Figure 3 shows a HRTEM image of an 8 nm-thick HfO_2/rutile TiO_2 (13 nm) stack film. The amorphous (a) and crystalline (c) regions are marked in Figure 3 for easy identification. In the ALD process of oxide materials at such low temperatures, the films generally begin to grow into an amorphous phase because of the insufficient thermal energy for the adsorbed atoms to move around on the surface. In addition, the interfacial energy between the crystalline film and substrate could be too high to crystallize the film from the beginning of film growth. As the film became thicker, the higher bulk free energy of the amorphous phase compared to that of the crystalline phase drives crystallization. This was observed for the HfO_2 ALD on Si and the thickness at which the structural change occurs depends on the types of the precursors.[15,16] For this BTEMAH precursor, the critical thickness was $\sim$18 nm on Si.[29] However, in this case, some parts of the HfO_2 film were crystallized in the early growth stage, suggesting that the interfacial energy between the HfO_2 crystal grain and the rutile TiO_2 is small enough to crystallize the HfO_2 films. For the thin films non-lattice matched with the substrate, the integral part of the interfacial energy was attributed mainly to lattice misfit between the film and substrate. The rutile TiO_2 film used as a substrate layer in this experiment has a [100] preferred orientation because the (200) plane of rutile TiO_2 could minimize the interfacial energy because of the small lattice

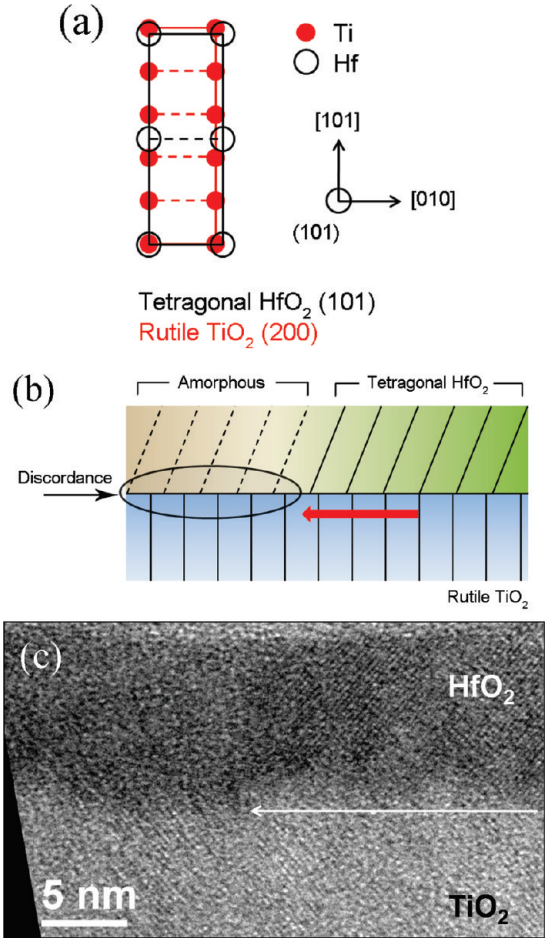

Figure 4. (a) Supercell structures of combined two unit cell of the tetragonal HfO_2 along the (101) plane (black rectangle) and combined five unit cell of rutile TiO_2 along the (200) plane (red rectangle). (b) Schematic diagram of limited crystallization of a tetragonal HfO_2 film on a large grain of rutile TiO_2 under-layer. (c) HRTEM image of a HfO_2 film on a single crystalline grain of a rutile TiO_2 film.

misfit with the RuO_2 substrate.[4,5] To understand the possible lattice match between rutile TiO_2 and tetragonal HfO_2, several major crystallographic planes of the two materials were compared. As a result, it was found that the vertices of combined two unit cells of tetragonal HfO_2 on the (101) plane could be matched to the vertices of the combined five unit cell of rutile TiO_2 (200) plane with relatively small lattice misfit. These supercell structures are shown schematically in Figure 4a. The lattice mismatch (δ) between the combined two unit cells of the tetragonal HfO_2 along the (101) plane and the combined five unit cells of rutile TiO_2 along the (200) plane are defined by $\delta_{H[101]} = (d_{T[010]} - d_{H[010]})/d_{H[010]}$, $\delta_{H[10\bar{1}]} = (5d_{T[001]} - 2d_{H[10\bar{1}]})/2d_{H[10\bar{1}]}$, where $d_{H[hkl]}$ and $d_{T[hkl]}$ are the unstressed interplanar spacing of the tetragonal HfO_2 (101) and rutile TiO_2 (200) planes along the [hkl] directions, respectively. The calculated $\delta_{H[010]}$ and $\delta_{H[110]}$ values were as small as -9.03% and 2.98%, respectively. This suggests that the tetragonal HfO_2 (101) plane on the rutile TiO_2 (200) plane can be energetically stable, and lead to the local epitaxial growth of tetragonal HfO_2 films on rutile TiO_2 films instead of forming a randomly oriented monoclinic HfO_2 phase. A similar lattice match

can barely be found between the tetragonal HfO_2 and anatase TiO_2 within a reasonable supercell structure.

However, the relatively large lattice mismatch, even with such a large supercell structure, may limit the lateral extension of the one tetragonal grain to quite limited dimensions, as shown schematically in Figure 4b. In Figure 4b, the substrate layer was assumed to have a single crystalline [200]-oriented TiO_2 considering the much larger grain size of TiO_2 compared to the crystallized HfO_2 grains. The lattice mismatch of 9.03% between HfO_2 and TiO_2 layers was considered in this case. When the crystalline seed of tetragonal HfO_2 was formed at a certain location on TiO_2 because of local lattice match and grows laterally to form the films (indicated by a red arrow in Figure 4b), the outer region of the crystalline grains has a higher interfacial energy because of the increasing lattice mismatch. Although the formation of dislocations and grain boundaries can reduce the stress induced by lattice mismatch,[31] they cannot relax sufficiently the stress in the HfO_2 film in this experiment because of the relatively large lattice mismatch. Therefore, the tetragonal HfO_2 is unstable and becomes amorphous at a certain amount of lattice mismatch. The amorphous region between the small crystal grains may relax the stress efficiently. This was observed experimentally, as shown in Figure 4c. The schematic structure in Figure 4b could not be confirmed directly because of the unfavorable orientation of the grains of TiO_2 and HfO_2 relative to the electron beam direction in the HRTEM. However, the crystalline structure of HfO_2 changes to an amorphous structure on a single TiO_2 grain, as indicated by the arrow in Figure 4c. The presence of grain boundaries of the rutile TiO_2 layer could also be a source of forming an amorphous region. Further structural analysis of the HfO_2 layer is discussed with the HRTEM images below.

Once this mixed structure of amorphous phase and columnar shaped crystal grains is formed during the initial growth of the film, as shown in Figure 3, it is difficult to crystallize the entire HfO_2 film, even when the film becomes thicker. There can be two possibilities for the change in HfO_2 film structure from a mixed structure to a fully crystalline structure as the film grows. One possibility is that both the amorphous and the tetragonal crystalline phases in the HfO_2 film become a monoclinic structure, which is the most stable structure under these experimental conditions. In this case, the crystalline structure of the tetragonal HfO_2 part should be rearranged. This process could be very slow because rather a high activation energy is needed to be overcome to induce a transformation from one crystal structure to another. The other possibility is that the only amorphous phase in the HfO_2 film is changed to a monoclinic structure. This route can be relatively easy because the grains of the preformed tetragonal phase can be retained during the transformation. However, the film after complete crystallization

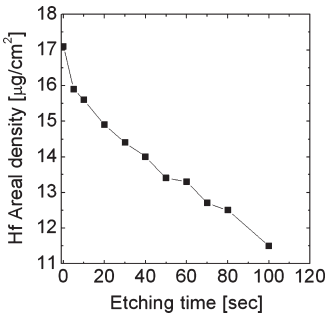

Figure 5. Changes in the Hf areal density of HfO_2/TiO_2 film as a function of the wet-etching time in a 1% HF water solution.

is believed to have a too high portion of interfaces between the tetragonal and the monoclinic phases because of the very small lateral size of the HfO_2 grains. To make this transformation possible, the HfO_2 film has to be much thicker to compensate for the high interfacial energy. For these reasons, the HfO_2 films deposited on rutile TiO_2 films could maintain the mixed structure of amorphous and tetragonal phases. The mixture structure of the HfO_2 film was confirmed by the change in Hf areal density measured by XRF and surface roughness measured by AFM after wet-etching as shown below.

Figure 5 shows the change in the Hf areal density of the HfO_2/rutile TiO_2 stack as a function of the wet-etching time in a 1% HF solution. Here, the HfO_2 film was originally 25 nm thick, and the TiO_2 film was not etched by this HF solution. The crystallinity of the HfO_2 films can be checked easily using this wet etching process because crystalline HfO_2 films are barely etched away whereas amorphous HfO_2 films are well etched.[32] It is obvious that the HfO_2 film contains an amorphous phase from the decrease in Hf layer density with respect to the wet etching time. The surface morphology of the as-deposited and wet-etched HfO_2 films was analyzed by AFM. Figure 6a,b shows AFM images of the as-deposited HfO_2 film and wet-etched HfO_2 film for 100 s, respectively. The wet-etched film (root-mean-squared (rms) roughness: 3.6 nm) is quite rough compared to the as-deposited film (rms roughness: 1.4 nm). This AFM image is quite different from the AFM images after similar wet-etching of the fully amorphous HfO_2 films deposited on a Si substrate, which showed almost no change in surface roughness (data not shown). The film surface after etching has the appearance of dispersed grains, and the AFM image is consistent with the HRTEM image of tetragonal columnar grains in Figure 3. The mixture of amorphous and crystalline HfO_2 phases showed an interesting morphology after wet-etching because amorphous HfO_2 is easier to etch in a HF solution than tetragonal grains. Figure 6c shows the line profile of the image in Figure 6b. This line profile makes it clearer that the HfO_2 films were etched selectively and the as-deposited HfO_2 films had a mixed structure of amorphous phase and columnar shape of crystal grains.

Reciprocal lattice analysis was performed to identify the crystal structure of HfO_2 films clearly. Fast Fourier

(31) Porter, D. A.; Easterling, K. E. *Phase Transformations in Metals and Alloys*, 2nd ed.; CRC Press: Boca Raton, FL, 2004.

(32) Consiglio, S.; Papadatos, F.; Naczas, S.; Skordas, S.; Eisenbraun, E. T.; Kaloyeros, A. E. *J. Electrochem. Soc.* **2006**, *153*, F249.

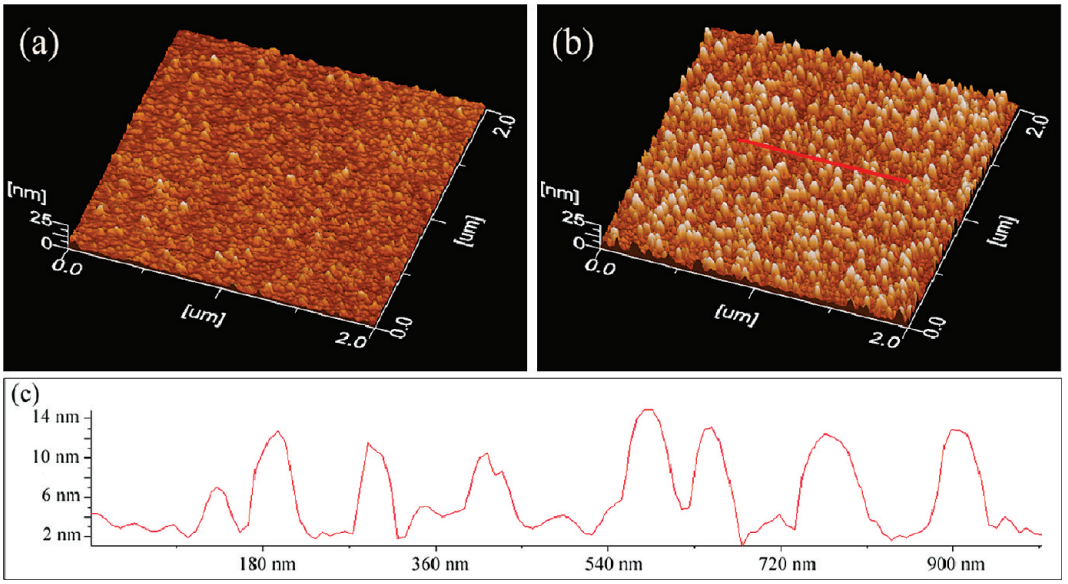

Figure 6. Three-dimensional AFM images of HfO_2 on a rutile TiO_2 film (a) before and (b) after the etching with HF solution. (c) Profile representing the cross section of a HfO_2/rutile TiO_2 film surface after etching with a HF solution.

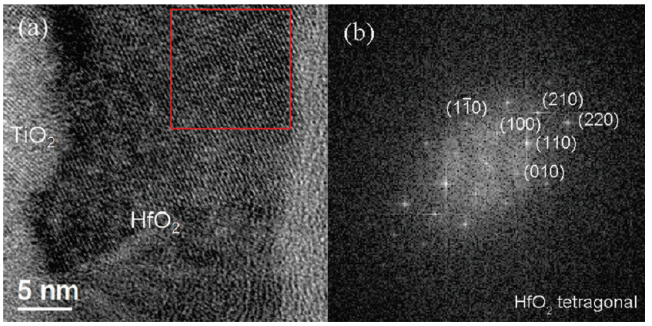

Figure 7. (a) HRTEM image of HfO_2 film on a rutile TiO_2 film. (b) Reciprocal lattice points of the square marked in panel a.

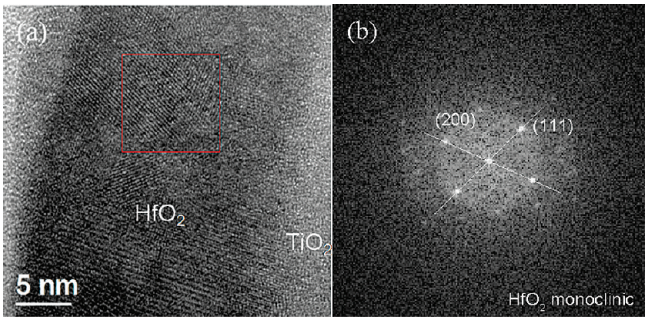

Figure 8. (a) HRTEM image of a HfO_2 film on an anatase TiO_2 film. (b) Reciprocal lattice points of the marked square in panel a.

transformation (FFT) was used to achieve the reciprocal lattice points from the HRTEM images. Figures 7a and 8a show HRTEM images of a 24 nm-thick HfO_2/rutile TiO_2 stack and HfO_2/anatase TiO_2 stack, respectively. There was also an attempt to correlate the relative crystallographic orientation of the crystalline HfO_2 grain and the underlying TiO_2, but the very different ion milling rates of HfO_2 and TiO_2 barely allowed an evenly thin enough region of both materials from the achievable TEM specimen.

The FFT images in Figures 7b and 8b correspond to the squared region in Figures 7a and 8a, respectively. The crystalline structure and crystalline face were determined from the distance between the reciprocal lattice points and center point and the angles between the two reciprocal lattice points from the converted reciprocal lattice points in the FFT images.[33] Consequently, an analysis of the reciprocal lattice showed that the HfO_2 film grown on the rutile TiO_2 layer had crystallized into a tetragonal structure, not a monoclinic structure. The crystalline face of the each point was marked with (*hkl*) in Figure 7b. On the other hand, the HfO_2 film grown on the anatase TiO_2 layer had fully crystallized, as shown in Figure 8a, and an analysis of the reciprocal lattice points in Figure 8b showed that the HfO_2 film has a monoclinic structure. The critical crystallization thickness for the monoclinic HfO_2 on Si was ~18 nm.[29] Therefore, the 24 nm-thick HfO_2 film on the non-lattice matched anatase TiO_2 was fully crystallized into the monoclinic structure. The TEM results show that the difference in k values in Figure 2 resulted from the difference in the crystalline structure of the HfO_2 films according to the crystalline structure of the TiO_2 substrate layer. Interestingly, the better lattice matched films showed partial crystallization, whereas the non-matched film showed a full crystallization.

The relative portion of the tetragonal HfO_2 part on rutile TiO_2 was 70% (from ~10 TEM images). Assuming the k value of amorphous phase as 16[34], the k value of the tetragonal HfO_2 was 35 ($16 \times 0.3 + 35 \times 0.7 = 29$), which is in reasonable coincidence with previous reports.[12−14]

Finally, the electrical performance of the tetragonal-amorphous HfO_2/rutile TiO_2 stacked layer was examined. Figure 9a shows the $J-V$ curves of the TiO_2 films and HfO_2/rutile TiO_2 stack films. The leakage current density of the HfO_2/rutile TiO_2 stack films was 100−10000

(33) Hirsch, P.; Howie, A.; Nicholson, R. B.; Pashley, D. W.; Whelan, M. J. *Electron Microscopy of Thin Crystals*, 2nd ed., Robert E. Krieger Publishing Co., Inc.: Malabar, FL, 1977.
(34) Vanderbilt, D.; Zhao, X.; Ceresoli, D. *Thin Solid Films* **2005**, *486*, 125.

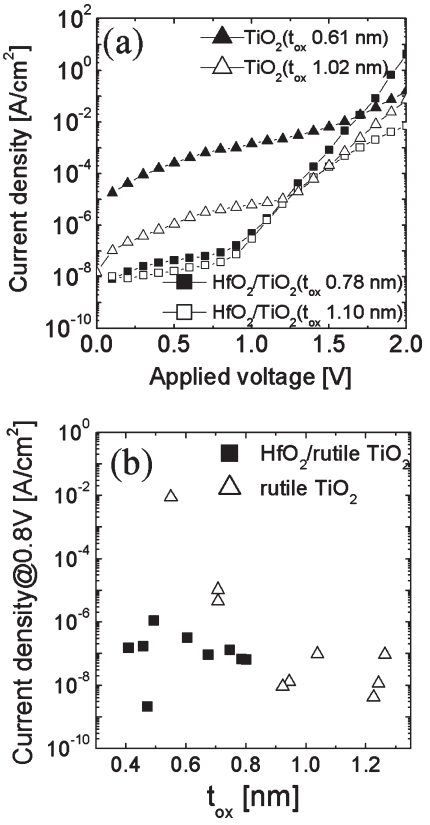

Figure 9. (a) $J-V$ curves of TiO_2/Ru and HfO_2/TiO_2/Ru stacks, (b) Overall summary plot of the J (at 0.8 V) versus t_{ox} of HfO_2/rutile TiO_2 stack films and TiO_2 films.

times lower than the J value of the TiO_2 single films under an applied voltage of 1.0 V, even though the t_{ox} values were similar. This means that the HfO_2 layer on the TiO_2 layer effectively suppresses the leakage current of the entire film stack. The mixed structure of HfO_2 films not only had a high k value, but also superiority in lowering the leakage current. Moreover, the HfO_2/rutile TiO_2 stack films can obtain an extremely small t_{ox} value because of the high k value of the tetragonal HfO_2 phase, which minimizes the t_{ox} sacrifice. From the overall summary plot of the J (at 0.8 V) versus t_{ox} in Figure 9 b, the HfO_2/rutile TiO_2 films show very low J values in a t_{ox} range of 0.4−0.8 nm, whereas the J values of TiO_2 films increased rapidly under a t_{ox} of 0.8 nm. Consequently, a t_{ox} of 0.41 nm was achieved with a J value of approximately 2×10^{-7} A/cm^2 at an applied voltage of 0.8 V from the 0.5 nm-thick HfO_2/6 nm-thick TiO_2 stacked film. This suggests that the HfO_2/rutile TiO_2 stack film is a very promising material as a capacitor dielectric for future generation DRAMs.

IV. Conclusions

HfO_2/rutile TiO_2 bilayered thin films were grown by ALD. The HfO_2 film grown on a rutile TiO_2 film showed a k value as high as 29, which is in contrast to only 16 for the HfO_2 films grown on the anatase TiO_2 film. It is believed that the structural compatibility of the specific plane of tetragonal HfO_2 with the rutile TiO_2 under-layer induced the formation of tetragonal structured HfO_2 films, even at such a low deposition temperature of 250 °C. The HfO_2 films deposited on the rutile TiO_2 under-layer showed a mixed structure of amorphous and tetragonal crystalline phases. The relatively large lattice mismatch between the tetragonal HfO_2 and rutile TiO_2 may induce misfit stress that is too large for a continuous tetragonal HfO_2 film to be produced. Therefore, a fine columnar structure of tetragonal HfO_2 grains with a dielectric constant of ~35 embedded in amorphous HfO_2 was achieved. On the other hand, a fully crystallized monoclinic HfO_2 film was achieved on the anatase TiO_2, which has virtually no crystallographic compatibility. An extremely small t_{ox} of 0.41 nm could be achieved with stable leakage properties using the tetragonal-amorphous HfO_2/rutile TiO_2 film. This is due to the minimized sacrifice of t_{ox} by adding the thin HfO_2 layer on the higher k TiO_2 and superior leakage current properties of thin HfO_2 film. The HfO_2/rutile TiO_2 stack film is a very promising high-k material with great synergy that supplements the weaknesses of each component.

Acknowledgment. This work was partly supported by the IT R&D program of MKE/KEIT [KI002178, Development of a mass production compatible capacitor for next generation DRAM], the Converging Research Center Program through the National Research Foundation of Korea (NRF) funded by the Ministry of Education, Science and Technology (2009-0081961), and World Class University program through the Korea Science and Engineering Foundation funded by the Ministry of Education, Science and Technology (R31-2008-000-10075-0).